

Training-Free Style and Content Transfer by Leveraging U-Net Skip Connections in Stable Diffusion

Anonymous CVPR submission

Paper ID 30

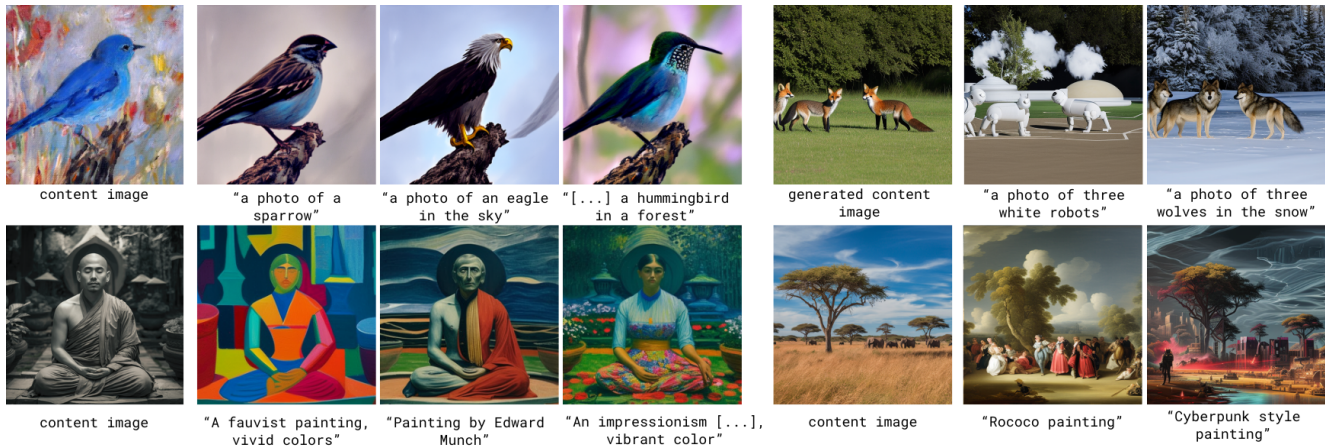


Figure 1. SkipInject: our method uses the $l=4$ and $l=5$ skip connections of Stable Diffusion to obtain flexible content and style transformations. From a painted “content image” of a bird, the model smoothly modifies the subject to resemble various species (e.g., sparrow, eagle) while retaining the overall scene. A generated image of foxes is transformed into “three white robots” and “three wolves in the snow,” with coherent and realistic alterations. Furthermore, the styles of the two content images are altered holistically, in aesthetics, subjects, and settings.

Abstract

alignment and optimal structural preservation tradeoff.

018

001 *Recent advances in diffusion models for image genera-*
 002 *tion have led to detailed examinations of several compo-*
 003 *nents within the U-Net architecture for image editing. While*
 004 *previous studies have focused on the bottleneck layer (h-*
 005 *space), cross-attention, self-attention, and decoding layers,*
 006 *the overall role of the skip connections of the U-Net it-*
 007 *self has not been specifically addressed. We conduct thor-*
 008 *ough analyses on the role of the skip connections and find*
 009 *that the residual connections passed by the third encoder*
 010 *block carry most of the spatial information of the recon-*
 011 *structed image, splitting the content from the style, passed*
 012 *by the remaining stream in the opposed decoding layer.*
 013 *We show that injecting the representations from this block*
 014 *can be used for text-based editing, precise modifications,*
 015 *and style transfer. We compare our method, SkipInject, to*
 016 *state-of-the-art style transfer and image editing methods*
 017 *and demonstrate that our method obtains the best content*

1. Introduction

019 Breakthroughs in diffusion models have unlocked unprecedented avenues for generating images and videos. Models such as Stable Diffusion [33], Midjourney, and Dall-E [31] have driven this evolution, with their outputs creating a transformative shift across diverse creative domains. Their influence reaches digital hobbyist circles, established professional practices like illustration, graphic design, and multimedia arts, and fosters innovative artistic exploration and community collaboration.

020 Despite the enormous generative affordances of these 020 methods, broader output controllability is necessary for better 021 adoption in creative communities, often reliant on a 022 trial-and-error process of iterative refinement and on mood 023 boarding and inspiration.

024 While previous generations of image generation mod-

025

026

027

028

029

030

031

032

033

034

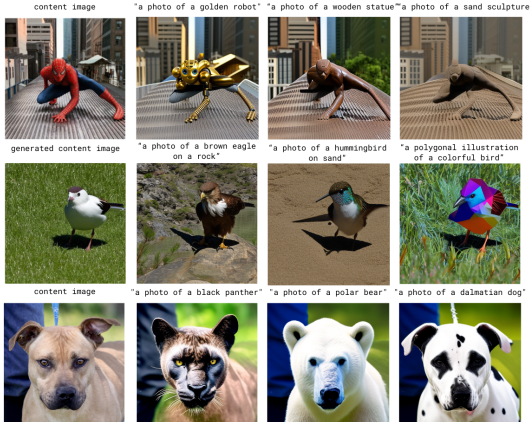


Figure 2. Examples of image editing results on Wild-TI2I and ImageNet-R-TI2I real and generated images.

els, including Variational Autoencoders [22] and Generative Adversarial Networks [20], leverage the latent space for image editing [14, 20, 37], diffusion models [16, 38] are based on a Markov chain denoising process and inherently lack a single latent space. In the context of U-Net-based diffusion models, training-free approaches to image editing focus on swapping different modules of the denoising architecture, including the self- and cross-attention modules and the h-space - the bottleneck of the U-Net. However, the skip connection - an essential element within the U-Net, aiding the transmission of long-range dependencies and the gradient propagation - has not been explored. In contrast to existing work, we focus on the former and its role in U-Net-based diffusion models.

To better understand the role of this module, we address the following questions: (i) How and where is information represented in the skip connections of the U-Net? (ii) How does it influence image generation? (iii) When does this information arise during the denoising process?

Interestingly, we observe that Stable Diffusion internally disentangles content from style within the third encoder/decoder block, with the content passing through the skip connection and the style through the main flow.

We find that injecting the third group of connections produced by the encoder from image A to image B transfers the spatial configuration of image A onto image B . Conversely, we find that image B transfers the style to image A using the same injection, indicating that the corresponding third decoder block carries the style information. Additionally, leveraging the injection timestep controls the appearance of the background of image B over image A , and modulating the mixing on the embedding offers control of the strength of the injection.

We demonstrate that an informed use of the properties of Stable Diffusion can achieve state-of-the-art performance on a wide variety of tasks, offering ample control over the

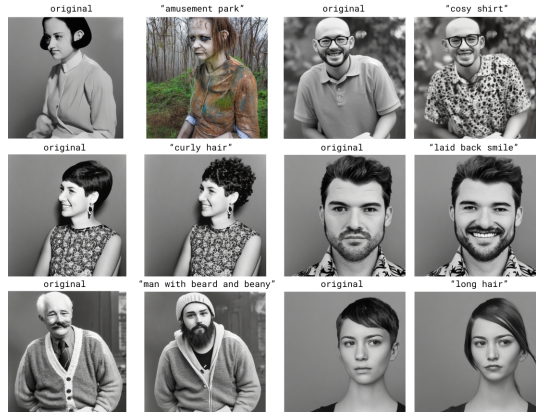


Figure 3. Image editing results on generated faces. We show precise transformations ranging from subtle changes, like makeup and hairstyle adjustments, to more global effects, including zombie-like effects. Our model preserves the core identity of each subject, maintaining facial structure.

intensity and nature of the output. In Sec. 5, we highlight the superiority of our method in achieving text-based image editing and style transfer and show preliminary results on fine-grained feature editing in Fig. 3.

To summarize, we contribute as follows:

- We investigate the role of the skip connections in the U-Net of Stable Diffusion, assessing their properties, their influence on the image, and variation across time steps.
- We propose an efficient and controllable image editing method and prove superiority or on-par SOTA performance on transferring content and style.
- Lastly, we propose three alternatives to modulate the editing effect.

2. Related work

In this section, we shortly explain the importance of latent space studies in the contexts of media studies and digital arts to further motivate the focus of this paper. Successively, we cover image editing methods on Stable Diffusion.

2.1. Latent space in the arts and humanities

The latent space, understood strictly as the space where the data lies in the bottleneck layer of a model, is a top-ical entity for studying and understanding models beyond technical fields. These spaces are studied as n-dimensional cultural objects [32]. The latent spaces make continuous and spatialized the cultural knowledge fed into or generated by the model, creating an implicit meaningful organization [36]. These representations can be then studied as a map of culture [43], and can, in turn, be used to study models as cultural snapshots of reality [7, 17, 44, 45].

Digital artists and creative industries extensively used latent space-rooted methodologies, such as latent space walks

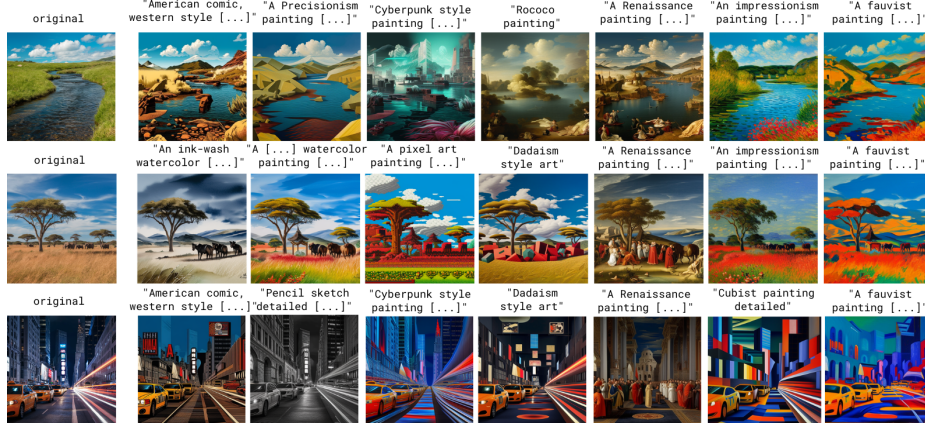


Figure 4. Examples of style transfer results on the Artist dataset [19].

102 and interpolation, to take advantage of the semantic
 103 continuity of this space. Initiating with DeepDream [2], the
 104 latent space continuity, opposed to reality’s fragmentation,
 105 creates an attractive space of artistic hallucination [1].

106 2.2. Image manipulation

107 In this section, we present some of the pivotal works in this
 108 direction, organized by what element is used for editing.

109 **Latent code-based editing.** Asyrrp [23] uses the *h-space*
 110 and CLIP supervision to find a direction of modification
 111 in the space at each timestep, to add to the original latent
 112 in the denoising process through a modified Diffusion De-
 113 terministic Implicit Model (DDIM) [39]. Boundary diffusion
 114 [48], on the other side, computes a modification direc-
 115 tion that is injected only at the mixing step, testing both ϵ -
 116 *space* and *h-space*. Haas *et al.* [11], among other findings,
 117 show that injecting the *h-space* of an image into another
 118 image changes the high-level semantics while retaining the
 119 structure and background. InjectFusion [18] observe the
 120 same phenomenon, implementing a calibrated procedure to
 121 inject the new *h-space*, maintaining the same correlation
 122 to the skip connections. These methods are mostly based
 123 on unconditional DDPM-based models trained on specific
 124 datasets for *e.g.* CelebA.

125 **Module-based editing.** Prompt2Prompt (P2P) [13] sub-
 126 stitute the cross-attentions of the U-Net layers to obtain
 127 text-based image editing. Plug and Play (PnP) [42] find
 128 that accurate editing can be achieved by injecting the spa-
 129 tial features of the middle decoding and self-attention lay-
 130 ers. Closely related to the two previous works, Liu *et*
 131 *al.* [24] investigate the role of the cross-attention and the
 132 self-attention in the different feature layers, observing again
 133 that intermediate features are the most salient. Finally,
 134 Artist [19] shows that using the middle residual blocks as
 135 PnP to control the content and the cross-attentions to inform
 136 the style obtains successful text-driven stylization.

137 **Text-based editing.** A common alternative for diffusion
 138 models leverages the manipulation of text conditioning.
 139 Methods like DiffusionCLIP [21] and InstructPix2Pix [4]
 140 fine-tune the model or the text conditioning to obtain de-
 141 sired edits. Various successful methods tackle personaliz-
 142 ing the outputs to specific entities such as Dreambooth [35].
 143 Lastly, methods like SDEdit [8] leverage partial inversion
 144 and text-guided generation to achieve fast, training-free
 145 editing.

146 **Adapters.** Other popular methods leverage adapters, in-
 147 cluding ControlNet [46] and T2IAdapter [27] to increase
 148 the modalities that can be used to control the diffusion pro-
 149 cess. In fact, they train an ad-hoc adapter for each addi-
 150 tional modality, obtaining perceptually interesting out-
 151 comes. To increase the manipulability, other methods make
 152 use of specifically trained LoRA adapters, like PreciseCon-
 153 trol [28] CTRLorALT [40], LoRAdapter [10], which can
 154 achieve controlled modifications for the trained semantic.

155 2.3. Novelty

156 Compared to existing methods, our approach is the simplest
 157 but allows the greatest control, using numerous plug-ins to
 158 modulate the effect and allowing, in the same pipeline, edit-
 159 ing the content and the style of the image. Lastly, we show
 160 that our method performs well on Turbo alternatives, ob-
 161 taining the fastest results.

162 3. Preliminaries

163 In this section, we introduce Latent Diffusion Models
 164 (LDMs) as introduced by Rombach *et al.* [33], with a par-
 165 ticular emphasis on its U-Net [34].

166 3.1. Latent Diffusion

167 Latent Diffusion Models (LDMs) overcome pixel-based
 168 diffusion models’ high computational and memory costs by
 169 conducting the diffusion process in a reduced latent space.

170 To achieve this, a pre-trained autoencoder converts an image into a compact latent representation z_0 of 1/8 the original per side size. The diffusion process is then applied to
 171 z_0 , which substantially lowers the resource demands during
 172 training and sampling. During training, the model is opti-
 173 mized to predict the noise via a neural network, the U-Net.
 174
 175

176 3.2. Components of the U-Net

177 In our work, we leverage a pre-trained text-conditioned Lat-
 178 ent Diffusion Model, which employs a U-Net backbone,
 179 popularly recognized as Stable Diffusion (versions 1.4, 1.5,
 180 2, and 2.1). In Stable Diffusion, the conventional U-Net archi-
 181 tecture [34] is enhanced with attention mechanisms, in-
 182 cluding self- and cross-attention blocks.

183 The **residual block** is inputted the latent features ϕ_t^{l-1}
 184 from the previous layer $l-1$ and outputs both the latent fea-
 185 tures to be inputted to the following block ϕ_t^l , and the skip
 186 connections f_t^l concatenated directly to the corresponding
 187 decoding layer, as:

$$188 f_t^l, \phi_t^l = \text{ResBlock}(\phi_t^{l-1}), \quad (1)$$

189 where ResBlock includes convolutional layers.

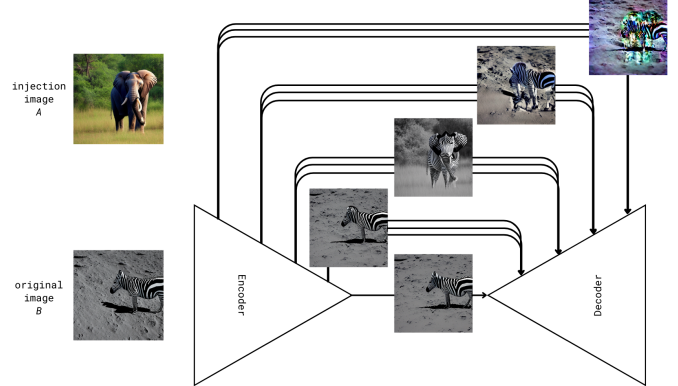
190 Stable Diffusion 1-2 models feature four encoding
 191 blocks, a bottleneck, and four mirroring decoding blocks.
 192 Each of the blocks contains three subblocks, each passing
 193 one skip connection. In the remainder of the paper, we re-
 194 fer to the skip connections by number, where $l=0$ is the
 195 first skip connection and $l=12$ is the one preceding the
 196 bottleneck.

197 4. Analysis

198 As explained in the previous section, skip connections are a
 199 critical component of the U-Net backbone, allowing long-
 200 range information flow and avoiding the vanishing gradient
 201 problem. However, their role within the Stable Diffusion
 202 models remains unknown. In this section, we present our
 203 investigation of the role of each skip connection, the time
 204 steps, and the properties of these embeddings to shed some
 205 light on these behaviors.

206 4.1. The role of skip connections

207 To analyze the effect of each skip connection, we store the
 208 skip connections of an injection image A and test the injec-
 209 tion of each skip connection and combinations of them into
 210 the original image B . We start from a common initial noise
 211 z_t . We follow two different noise selection strategies: (i)
 212 we randomly sample a z_t from a Gaussian distribution, or
 213 (ii) we use the result of the DDIM inversion of either A , i.e.,
 214 z_t^A , or B , i.e., z_t^B . We first fully denoise z_t with the prompt
 215 of image A , p^A , and store the skip connection f_t^l at each
 216 time-step t . Successively, we denoise z_t using the prompt
 217 of image B , p^B . At each time-step from t_{start} to t_{end} , we



218 Figure 5. Visualization of the effect of switching each group of
 219 skip connections. We show the result of each skip connection
 220 switched on the respective swapped group. We observe that the h -
 221 space has an almost imperceptible effect on the final image, con-
 222 trary to research into the disentanglement of DDPMs. The first
 223 group of skip connections closest to the h -space similarly has a
 224 limited effect, whereas the most coherent blending occurs in the
 225 second group of skip connections. The third group has no coher-
 226 ent effect on the image, generating random distortions, while the
 227 fourth performs akin to raw pixel blending.

228 substitute the skip connection f_t^l of image A . We show an
 229 example of the effect we obtain by substituting each group
 230 of three skip connections (group 1: $l=1,2,3$; group 2:
 231 $l=4,5,6$; group 3: $l=7,8,9$; group 4: $l=10,11,12$)
 232 and the h -space in Fig. 5.

233 Previous studies [19, 24, 42] indicate that the middle de-
 234 coding layers or the middle cross- and self-attention blocks
 235 are the most determinant of the content, suggesting that
 236 the structural information is formed roughly halfway in the
 237 decoding blocks. While our method aligns with previous
 238 findings, being the third group of skip connections roughly
 239 halfway in the depth of the model, it suggests that this in-
 240 formation is already encoded in the encoder and passed
 241 through the decoder via the residual block.

242 Accepting standard distinctions of foreground-
 243 background and content-style¹, we observe that the
 244 injection of the second group of skip connections of image
 245 A into image B preserves the background style of image
 246 B , in this case, the color scheme, the foreground style of
 247 image B , the stripes of the zebra, the background content
 248 of image A , the Savannah, and the foreground content of
 249 image A , the silhouette of the elephant.

250 4.2. The effect of the timesteps

251 In this section, we investigate the role of timesteps in the
 252 diffusion process (see Fig. 7) by injecting the skip connec-
 253

254 ¹While these terms do not have a precise definition, by content, we
 255 generally mean the structure of the object, and by style, the colors, textures,
 256 and patterns.

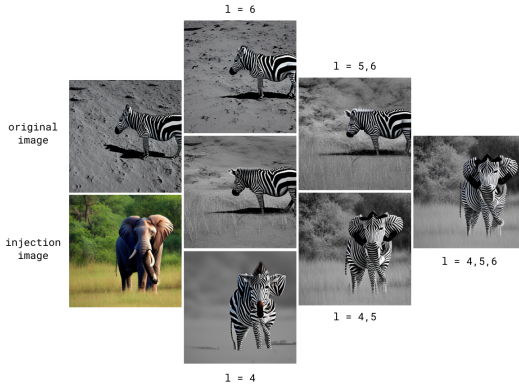


Figure 6. Close up into the second group of skip connections. The image shows the effect of this group’s different combinations of connections. From the bottom to the top, we injected only one of the skip connections, groups of two, and finally, all three. Specifically, we observe that the combination of $l = 4$ and $l = 5$ carry the most information: $l = 5$ injected alone creates a minimal change in the image but, when combined with $l = 4$, determines the spatial structure of the output. $l = 4$ alone conveys structure only of the foreground.

243 tion of image A into image B at $t_{start} \neq 1000$ and $t_{end} \neq 0$.
 244 We observe that the first 150 steps ($t_{start} = 850$) have
 245 little impact on the final image, while the last 150 steps
 246 ($t_{end} = 150$) only serve as refinement, as found also in
 247 Asyrp [23]. We find that the skip connection of image A
 248 or image B for the first 500 denoising steps determines the
 249 content of the foreground, while the last 500 steps deter-
 250 mine the background.

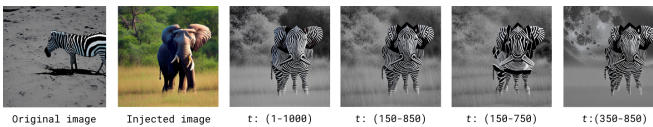


Figure 7. Visualization of the effect of the injection timesteps. We observe that starting the injection later at $t_{start} < 850$ leads to distortions in the foreground content while ending the denoising earlier at $t_{end} > 150$ reveals the background content of the original image. This phenomenon is consistent for every image we generate.

4.3. Modulating the effect

To achieve more controllable results, we investigate methods to modulate the intensity of the change.

Injection classifier-free guidance. Inspired by classifier-free guidance [15], we test the use of a linear combination of the injected embedding and original embedding of the changed skip connections, parametrized by γ to balance the intensity of the mix. At each denoising step, the

injected embedding becomes:

$$f^A(t, l) = f^B(t, l) + \gamma(f^A(t, l) - f^B(t, l)) \quad (2) \quad 260$$

where t is the denoising timestep and l the skip connection layer.

Depth-wise alternation of the spatial embedding of the skip connections. The h -space and each skip connection are high-dimensional matrices with depth, width, and height channels. For instance, the layer $l = 4$ for a 512×512 output size is $1280 \times 16 \times 16$, so $depth = 1280$ and $width = height = 16$, as opposed to traditional latent spaces of GANs and VAEs of size 512. We hypothesize that the information stored in these embeddings is, therefore, highly redundant and attempt to investigate the nature of these spaces' spatial features (width and height). We plot these embeddings as 1280 images of 16×16 pixels and we find that over 90% of the kernels show the same shape with varying average or inverse intensities. Therefore, we suspect redundancy in the depth channel.

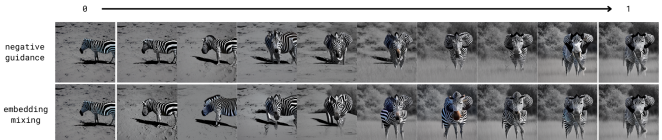


Figure 8. Visualization of modulation methods. We show the effects of the two modulation methods at $\gamma = r \in [0, 1]$. We observe that both methods achieve a successful modulation of the intensity of the effect and empirically observe that the use of both methods together obtains the best results. The advantage of the guidance is that it can surpass the effect above 1, but, differently from the second modulation method, it struggles in areas around 1, where the image should be similar to the non-modulated effect.

We leverage this observation to introduce an additional modulation method: we alternate at a ratio r the kernels of $f^A(t, l)$ with those of $f^B(t, l)$. That is to say, for every $1280 \times r$ 16×16 kernels, we inject the injection kernel and maintain the original one in the other cases.

In sum, the injection timing can control whether the background is retained or replaced with that of the original image, and the injection strength can be further modulated using classifier-free guidance and depth-channel alternation.

5. Experiments

We evaluate our method on **image editing** and **style transfer**, providing both quantitative metrics and qualitative results. To evaluate our method on text-guided image-to-image and text-to-image translation, we follow established benchmarks, utilizing the Wild-TI2I dataset [42] and ImageNet-R-TI2I [42]. We adopt the protocol outlined in



Figure 9. Qualitative comparison of different prompt-guided editing methods. We use as reference results proposed by [24] thus, we do not cherry-pick the results. From left to right: source image, target prompt, our result, Free Prompt Editing, P2P [12], PnP [41], SDEdit [26] with two noise levels, DiffEdit [9], Pix2pixzero [25], Shape-guided [29], MasaCntrl [5], and InstructPix2Pix [3] (a fine-tuning-based method).

294 [19] for style transfer evaluation to text-guided style transfer.
295

296 Our evaluation employs two complementary metrics.
297 First, text-image CLIP similarity quantifies how closely the
298 generated images align with the style or edit prompts [30].
299 Second, the distance between DINO ViT self-similarity [6]
300 assesses the degree of structure preservation. Additionally,
301 we use LPIPS [47] to measure perceptual similarity, where
302 lower values indicate better content retention.

303 We implement our method with the Diffusers
304 library, using a custom 2DUNetConditional
305 model based on pre-trained weights from
306 stabilityai/stable-diffusion-2-base.
307 For image-to-image translation, we apply the
308 DDIMInverseScheduler with 50 steps, generating
309 images with the UniPCMultistepScheduler
310 using 50 inference steps and a guidance scale of 7.5.
311
cd

312 5.1. Image editing

313 **Qualitative Analysis** provides a comparative analysis with
314 previous methods. Competing methods frequently exhibit
315 issues: Free Prompt Editing lacks style specificity (e.g.,
316 "penguin embroidery" fails to capture the embroidery tex-
317 ture), Prompt2Prompt does not follow the prompt effec-
318 tively (the horse is not in the museum), and Plug-and-Play
319 leads to feature distortions (e.g., "silver robot"). SDEdit
320 struggles with structural integrity at high noise levels, while
321 DiffEdit and MaCaCntrl lose context (e.g., the "teddy bear"
322 is distorted). In contrast, our model consistently deliv-
323 ers prompt-specific transformations with high structural fi-

324 delity, demonstrating robustness across various styles and
325 editing demands.

326 **Quantitative analysis** Quantitatively, we present the per-
327 formance of our methods on the ImageNet-R-TI2I and
328 Wild benchmarks. In Fig 10 we evaluate our model with
329 CLIP cosine similarity (indicating prompt fidelity) and
330 DINO-ViT self-similarity (indicating structural preserva-
331 tion). Across all benchmarks (Wild-TI2I, ImageNet-R-
332 TI2I, and Generated ImageNet-R-TI2I), our model con-
333 stantly balances high CLIP similarity with low DINO
334 self-similarity, outperforming other methods like SDEdit,
335 VQGAN-CLIP, and DiffuseIT in both text alignment and
336 structural accuracy. Notably, our approach consistently
337 places in the "Better" region, reflecting superior text fidelity
338 and structural integrity.

339 5.2. Style Transfer

340 **Qualitative evaluation** Figure 11 offers a comparative
341 analysis, highlighting distinctive performance variations
342 among competing models. Models like DiffStyler, CLIP-
343 Styler, and Plug-and-Play often compromise the fidelity of
344 the original content structure, leading to blurred or distorted
345 shapes, particularly in intricate or highly abstract styles.
346 NTI+P2P exhibits minimal style alteration, evident in the
347 "8-bit pixel art" transformation, where the ship closely re-
348 sembles the original. However, it is relevant to note that
349 while these models demonstrate varying degrees of style
350 application, evaluating artistic styles can be inherently arbi-
351 trary. Styles intended as artistic movements are sometimes
352 conflated with specific methods, making objective assess-
353 ment challenging. For instance, applying a "Dadaism style"

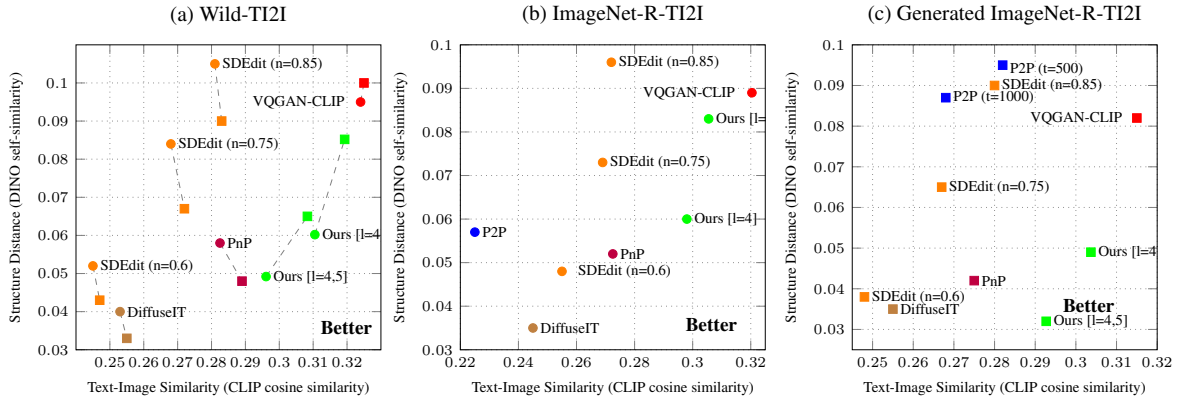


Figure 10. Quantitative evaluation. We measure CLIP cosine similarity (higher is better) and DINO-ViT self-similarity distance (lower is better) to quantify the fidelity to text and preservation of structure, respectively. We report these metrics on three benchmarks: (a) Wild-TI2I, (b) ImageNet-R-TI2I, and (c) Generated ImageNet-R-TI2I. [42]



Figure 11. Qualitative evaluation against current style transfer methods. We use the reference results by [19], and we do not do any cherry-picking.

354 prompt may focus on collage techniques rather than capturing
355 the movement’s conceptual essence.

356 In contrast, our model achieves a balanced and coher-
357 ent output across styles, effectively preserving not only the
358 content structure and the stylistic features but also adjusting
359 the people, clothing, and objects in a historically coherent
360 manner (as in Fig. 11). For example, in the “Impressionist
361 painting” transformation, our model accurately replicates
362 the brushstroke aesthetic and introduces a poppy field, typi-
363 cal of Impressionist painters, while maintaining the original
364 shape and posture of the horse. Nonetheless, our method in-
365 herits certain biases from Stable Diffusion, resulting in in-
366 accurate visual aesthetics for movements like Cubism, Fu-
367 turism, and Dadaism despite successfully achieving stereo-
368 typical modifications.

369 In Fig. 12, we show a practical application of the style
370 transfer features of our model, demonstrating interesting ap-
371 plicability to styles presented by the creative communities
372 adopting Midjourney and StabilityAI using both a prompt
373 and an image for style transfer. Note that the latter has not
374 been shown to work for competing works.

375 **Quantitative evaluation** Our method, represented by **l=4,5**

376 and **l=4** in Table 1, demonstrates strong alignment with text
377 prompts while preserving content structure. On the CLIP
378 Alignment metric, the **l=4** model achieves the highest score
379 of 28.55, with **l=4,5** close behind at 26.27. These scores
380 indicate that our model adheres effectively to prompt guid-
381 ance, achieving transformations that accurately reflect the
382 target style. Regarding structural similarity, our **l=4,5** model
383 attains an LPIPS score of 0.57, with **l=4** following at 0.67,
384 demonstrating good content retention compared to most
385 baseline models. These lower LPIPS values suggest that
386 our approach maintains structural and perceptual fidelity to
387 the original content, even under significant stylistic trans-
388 formations. Competing methods, such as DDIM (0.74), Diff-
389 Styler (0.72), and ControlNet-Depth (0.78), display higher
390 LPIPS scores, reflecting a greater degree of content distor-
391 tion. Artist shows competing performance while obtaining
392 inferior qualitative results.

393 Finally, in Fig. 13, we show the impressive editing re-
394 sults achieved on the turbo-distilled version of the model.
395 Previous works have not shown this applicability.

Table 1. Evaluation of Different Style Transfer Models on the Artist Dataset [19], measuring Content Preservation (LPIPS) and Stylization Prompt Alignment (CLIP Alignment).

Metric	Ours (l=4,5)	Ours (l=4)	Artist	DDIM	NTI-P2P	PnP	DiffStyler	InstructP2P	ControlNet-Canny	ControlNet-Depth	CLIPStyler
LPIPS ↓	0.57	0.67	0.62	0.74	0.67	0.67	0.72	0.47	0.72	0.78	0.51
CLIP Alignment ↑	26.27	28.55	28.33	28.38	25.87	26.4	26.82	23.59	26.4	27.05	26.14

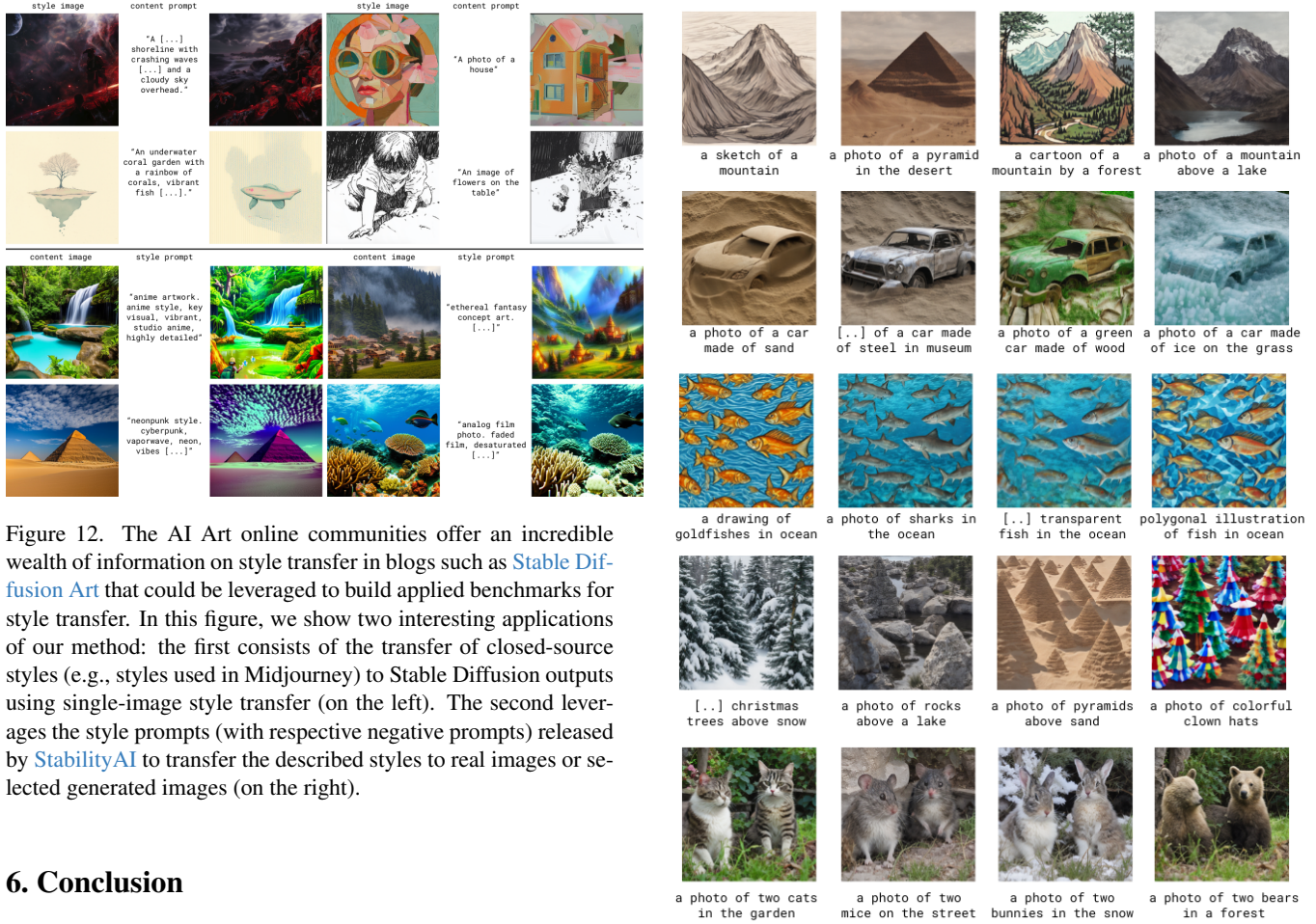


Figure 12. The AI Art online communities offer an incredible wealth of information on style transfer in blogs such as [Stable Diffusion Art](#) that could be leveraged to build applied benchmarks for style transfer. In this figure, we show two interesting applications of our method: the first consists of the transfer of closed-source styles (e.g., styles used in Midjourney) to Stable Diffusion outputs using single-image style transfer (on the left). The second leverages the style prompts (with respective negative prompts) released by [StabilityAI](#) to transfer the described styles to real images or selected generated images (on the right).

396

6. Conclusion

397 In conclusion, this paper explores the impact of U-Net
 398 skip connections in Stable Diffusion models, presenting a
 399 training-free, efficient approach - SkipInject - that enables
 400 high-quality text-guided image editing and style transfer.
 401 By systematically examining these skip connections, we ad-
 402 dress key questions about how spatial and stylistic infor-
 403 mation is encoded in the latent spaces of Stable Diffusion, the
 404 stages within the denoising process where they arise, and
 405 the structure of these spaces. Our findings reveal that spe-
 406 cific skip connections are fundamental in controlling con-
 407 tent and style, providing insight into how these components
 408 influence image generation.

409 The proposed method leverages the l=4 and l=5 skip
 410 connections to achieve precise style and content transfer,
 411 demonstrating state-of-the-art or on-par performance across
 412 established benchmarks. In addition, we introduce three
 413 modulation techniques for controlled editing intensity, of-

Figure 13. Example results of text-based image editing using Stable Diffusion Turbo with 1 step inference on `wild-ti2i-fake`. The modifications obtained are coherent and cohesive, obtaining radical changes and maintaining the original structure. Compared to multi-step inference, the control over the background is more limited.

fering flexible adjustments to meet diverse requirements.

Our approach currently relies on a single latent, limiting its application from scenarios that require dual-image style transfer. Future work will focus on extending SkipInject to support two-image inputs for broader applications.

414

415

416

417

418

419 **References**

420 [1] Art walks in latent spaces, . 3

421 [2] Inceptionism: Going Deeper into Neural Networks, . 3

422 [3] Tim Brooks, Aleksander Holynski, and Alexei A Efros. In- 423 structpix2pix: Learning to follow image editing instructions. In 424 *Proceedings of the IEEE/CVF Conference on Computer 425 Vision and Pattern Recognition*, pages 18392–18402, 2023. 426 6

427 [4] Tim Brooks, Aleksander Holynski, and Alexei A. Efros. In- 428 structPix2Pix: Learning To Follow Image Editing Instructions. 429 pages 18392–18402, 2023. 3

430 [5] Mingdeng Cao, Xintao Wang, Zhongang Qi, Ying Shan, Xi- 431 aohu Qie, and Yinqiang Zheng. Masactrl: Tuning-free mu- 432 tual self-attention control for consistent image synthesis and 433 editing. In *Proceedings of the IEEE/CVF International 434 Conference on Computer Vision*, pages 22560–22570, 2023. 6

435 [6] Mathilde Caron, Hugo Touvron, Ishan Misra, Hervé Jégou, 436 Julien Mairal, Piotr Bojanowski, and Armand Joulin. Emerg- 437 ing properties in self-supervised vision transformers. In *Pro- 438 ceedings of the IEEE/CVF international conference on com- 439 puter vision*, pages 9650–9660, 2021. 6

440 [7] Eva Cetinic. The Myth of Culturally Agnostic AI Models, 441 2022. arXiv:2211.15271 [cs]. 2

442 [8] Paramanand Chandramouli. LDEdit: Towards Generalized 443 Text Guided Image Manipulation via Latent Diffusion 444 Models. 3

445 [9] Guillaume Couairon, Jakob Verbeek, Holger Schwenk, 446 and Matthieu Cord. Diffedit: Diffusion-based seman- 447 tic image editing with mask guidance. *arXiv preprint 448 arXiv:2210.11427*, 2022. 6

449 [10] Rohit Gandikota, Joanna Materzynska, Tingrui Zhou, 450 Antonio Torralba, and David Bau. Concept Sliders: LoRA 451 Adaptors for Precise Control in Diffusion Models, 2023. 452 arXiv:2311.12092 [cs]. 3

453 [11] René Haas, Inbar Huberman-Spiegelglas, Rotem Mulay- 454 off, Stella Graßhof, Sami S. Brandt, and Tomer Michaeli. 455 Discovering Interpretable Directions in the Semantic Latent 456 Space of Diffusion Models, 2023. 3

457 [12] Amir Hertz, Ron Mokady, Jay Tenenbaum, Kfir Aberman, 458 Yael Pritch, and Daniel Cohen-Or. Prompt-to-prompt im- 459 age editing with cross attention control. *arXiv preprint 460 arXiv:2208.01626*, 2022. 6

461 [13] Amir Hertz, Ron Mokady, Jay Tenenbaum, Kfir Aberman, 462 Yael Pritch, and Daniel Cohen-Or. Prompt-to- 463 Prompt Image Editing with Cross Attention Control, 2022. 464 arXiv:2208.01626 [cs]. 3

465 [14] Irina Higgins, Loic Matthey, Arka Pal, Christopher Burgess, 466 Xavier Glorot, Matthew Botvinick, Shakir Mohamed, and 467 Alexander Lerchner. beta-VAE: Learning Basic Visual 468 Concepts with a Constrained Variational Framework. 2016. 2

469 [15] Jonathan Ho and Tim Salimans. Classifier-Free Diffusion 470 Guidance. 2021. 5

471 [16] Jonathan Ho, Ajay Jain, and Pieter Abbeel. Denoising 472 Diffusion Probabilistic Models, 2020. arXiv:2006.11239 [cs, 473 stat]. 2

474 [17] Leonardo Impett and Fabian Offert. There Is a Digital Art 475 History, 2023. arXiv:2308.07464 [cs]. 2

476 [18] Jaeseok Jeong, Mingi Kwon, and Youngjung Uh. Training- 477 Free Content Injection Using H-Space in Diffusion Models. 478 pages 5151–5161, 2024. 3

479 [19] Ruixiang Jiang and Changwen Chen. Artist: Aesthetically 480 Controllable Text-Driven Stylization without Training, 2024. 481 arXiv:2407.15842 [cs]. 3, 4, 6, 7, 8

482 [20] Tero Karras, Samuli Laine, and Timo Aila. A Style- 483 Based Generator Architecture for Generative Adversarial 484 Networks. pages 4401–4410, 2019. 2

485 [21] Gwanghyun Kim, Taesung Kwon, and Jong Chul Ye. Diffu- 486 sionCLIP: Text-Guided Diffusion Models for Robust Image 487 Manipulation. In *2022 IEEE/CVF Conference on Computer 488 Vision and Pattern Recognition (CVPR)*, pages 2416–2425, 489 New Orleans, LA, USA, 2022. IEEE. 3

490 [22] Diederik P. Kingma and Max Welling. Auto-Encoding 491 Variational Bayes, 2022. arXiv:1312.6114 [cs, stat]. 2

492 [23] Mingi Kwon, Jaeseok Jeong, and Youngjung Uh. Diffu- 493 sion Models already have a Semantic Latent Space, 2023. 494 arXiv:2210.10960 [cs]. 3, 5

495 [24] Bingyan Liu, Chengyu Wang, Tingfeng Cao, Kui Jia, and Jun 496 Huang. Towards Understanding Cross and Self-Attention 497 in Stable Diffusion for Text-Guided Image Editing, 2024. 498 arXiv:2403.03431 version: 1. 3, 4, 6

499 [25] Matthew Martinez, Steven Hernandez, Joseph Davis, 500 William Rodriguez, and Paul Lopez. Introducing pix2pix- 501 zero: Efficient and effective zero-shot image-to-image trans- 502 lation with diffusion models. 6

503 [26] Chenlin Meng, Yutong He, Yang Song, Jiaming Song, Jia- 504 jun Wu, Jun-Yan Zhu, and Stefano Ermon. Sdedit: Guided 505 image synthesis and editing with stochastic differential equa- 506 tions. *arXiv preprint arXiv:2108.01073*, 2021. 6

507 [27] Chong Mou, Xintao Wang, Liangbin Xie, Yanze Wu, Jian 508 Zhang, Zhongang Qi, Ying Shan, and Xiaohu Qie. T2I- 509 Adapter: Learning Adapters to Dig out More Control- 510 lable Ability for Text-to-Image Diffusion Models, 2023. 511 arXiv:2302.08453. 3

512 [28] Rishabh Parihar, Sachidanand VS, Sabariswaran Mani, Te- 513 jan Karmali, and R. Venkatesh Babu. PreciseControl: En- 514 hancing Text-To-Image Diffusion Models with Fine-Grained 515 Attribute Control, 2024. arXiv:2408.05083 [cs]. 3

516 [29] Dong Huk Park, Grace Luo, Clayton Toste, Samaneh Azadi, 517 Xihui Liu, Maka Karalashvili, Anna Rohrbach, and Trevor 518 Darrell. Shape-guided diffusion with inside-outside atten- 519 tion. In *Proceedings of the IEEE/CVF Winter Conference on 520 Applications of Computer Vision*, pages 4198–4207, 2024. 6

521 [30] Alec Radford, Jong Wook Kim, Chris Hallacy, Aditya 522 Ramesh, Gabriel Goh, Sandhini Agarwal, Girish Sastry, 523 Amanda Askell, Pamela Mishkin, Jack Clark, et al. Learning 524 transferable visual models from natural language supervi- 525 sion. In *International conference on machine learning*, pages 526 8748–8763. PMLR, 2021. 6

527 [31] Aditya Ramesh, Prafulla Dhariwal, Alex Nichol, Casey Chu, 528 and Mark Chen. Hierarchical Text-Conditional Image Gen- 529 eration with CLIP Latents, 2022. arXiv:2204.06125. 1

530 [32] Nuria Rodríguez-Ortega. Techno-Concepts for the Cultural 531 Field: n-Dimensional Space and Its Conceptual Constella- 532 tion. *Multimodal Technologies and Interaction*, 6(11):96, 533 2022. 2

534 [33] Robin Rombach, Andreas Blattmann, Dominik Lorenz,
535 Patrick Esser, and Björn Ommer. High-Resolution Image
536 Synthesis With Latent Diffusion Models. pages 10684–
537 10695, 2022. 1, 3

538 [34] Olaf Ronneberger, Philipp Fischer, and Thomas Brox. U-
539 Net: Convolutional Networks for Biomedical Image Seg-
540 mentation, 2015. arXiv:1505.04597 [cs]. 3, 4

541 [35] Nataniel Ruiz, Yuanzhen Li, Varun Jampani, Yael Pritch,
542 Michael Rubinstein, and Kfir Aberman. DreamBooth: Fine
543 Tuning Text-to-Image Diffusion Models for Subject-Driven
544 Generation. pages 22500–22510, 2023. 3

545 [36] Nick Seaver. Everything lies in a space: cultural
546 data and spatial reality. *Journal of the Royal An-*
547 *thropological Institute*, 27(S1):43–61, 2021. *reprint*:
548 <https://onlinelibrary.wiley.com/doi/pdf/10.1111/1467-9655.13479>. 2

549 [37] Yujun Shen, Ceyuan Yang, Xiaou Tang, and Bolei Zhou.
550 InterFaceGAN: Interpreting the Disentangled Face Repre-
551 sentation Learned by GANs. *IEEE Transactions on Pattern*
552 *Analysis and Machine Intelligence*, 44(4):2004–2018, 2022.
553 Conference Name: IEEE Transactions on Pattern Analysis
554 and Machine Intelligence. 2

555 [38] Jascha Sohl-Dickstein, Eric A. Weiss, Niru Mah-
556 eswaranathan, and Surya Ganguli. Deep Unsupervised
557 Learning using Nonequilibrium Thermodynamics, 2015.
558 arXiv:1503.03585. 2

559 [39] Jiaming Song, Chenlin Meng, and Stefano Ermon. Denois-
560 ing Diffusion Implicit Models, 2022. arXiv:2010.02502 [cs].
561 3

562 [40] Nick Stracke, Stefan Andreas Baumann, Joshua M.
563 Susskind, Miguel Angel Bautista, and Björn Ommer. CTR-
564 LorALTer: Conditional LoRAdapter for Efficient 0-Shot
565 Control & Altering of T2I Models, 2024. arXiv:2405.07913
566 [cs]. 3

567 [41] Narek Tumanyan, Michal Geyer, Shai Bagon, and Tali
568 Dekel. Plug-and-play diffusion features for text-driven
569 image-to-image translation. In *Proceedings of the IEEE/CVF*
570 *Conference on Computer Vision and Pattern Recognition*,
571 pages 1921–1930, 2023. 6

572 [42] Narek Tumanyan, Michal Geyer, Shai Bagon, and Tali
573 Dekel. Plug-and-Play Diffusion Features for Text-Driven
574 Image-to-Image Translation. pages 1921–1930, 2023. 3, 4,
575 5, 7

576 [43] Ted Underwood. Mapping the Latent Spaces of Culture.
577 2021. 2

578 [44] Ted Underwood and Richard Jean So. Can We Map Culture?
579 *Journal of Cultural Analytics*, 6(3), 2021. 2

580 [45] Max Weisbuch, Sarah A. Lamer, Evelyne Treinen,
581 and Kristin Pauker. Cultural snapshots: The-
582 ory and method. *Social and Personality Psy-*
583 *chology Compass*, 11(9):e12334, 2017. *reprint*:
584 <https://onlinelibrary.wiley.com/doi/pdf/10.1111/spc3.12334>.
585 2

586 [46] Lvmin Zhang, Anyi Rao, and Maneesh Agrawala. Adding
587 Conditional Control to Text-to-Image Diffusion Models,
588 2023. arXiv:2302.05543 [cs]. 3

589 [47] Richard Zhang, Phillip Isola, Alexei A Efros, Eli Shecht-
590 man, and Oliver Wang. The unreasonable effectiveness of
591 deep features as a perceptual metric. In *Proceedings of the*
592 *IEEE conference on computer vision and pattern recogni-*
593 *tion*, pages 586–595, 2018. 6

594 [48] Ye Zhu, Yu Wu, Zhiwei Deng, Olga Russakovsky, and Yan
595 Yan. Boundary Guided Learning-Free Semantic Control
596 with Diffusion Models, 2023. arXiv:2302.08357 [cs]. 3

597